Improvement of adjoint based methods for efficient computation of response surfaces

By F. Palacios†, K. Duraisamy AND J. J. Alonso

1. Motivation and objectives

In computational fluid dynamics, the solution of the dual (or adjoint) equations in conjunction with the primal (or flow equations) offers valuable information that can be used in design, sensitivity analysis, error estimation, mesh adaptation, uncertainty quantification, etc. From the view point of implementation and application of the adjoint technique, one of the following two approaches may be pursued: the continuous method and the discrete one. In the continuous approach (Jameson 1988; Anderson & Venkatakrishnan 1997; Kim *et al.* 2002; Castro *et al.* 2007), the adjoint equations are derived from the continuous flow equations and then subsequently discretized using a numerical method of choice, whereas in the discrete approach (Griewank 2000; Nadarajah & Jameson 2000; Giles *et al.* 2003; Mavriplis 2006; Mader *et al.* 2008), the adjoint equations are directly derived from the discretized governing equations. These approaches offer distinct advantages in different scenarios and have both been implemented for purposes of Verification and Validation (V&V) and Uncertainty Quantification (UQ) in hypersonic flow applications. In this work, we outline preliminary work in two areas of research that involve the use of adjoints in uncertainty quantification:

• Uncertainty quantification using non-intrusive methods such as stochastic collocation (Eldred 2009) typically involves the construction of a response surface of the quantity of interest as a function of the uncertain parameters. To achieve the level of desired accuracy, a large number of Computational Fluid Dynamics (CFD) simulations is typically required. To improve the efficiency of this process, we propose a new "robust" grid adaptation technique that is aimed at minimizing the numerical error over a small variation of the parameters around a nominal state. In this approach, computational grids are generated with the knowledge that small variations of the uncertain parameters can locally change the solution (and hence, the error distribution). This is in contrast to classical adjoint techniques (Pierce & Giles 2002; Fidkowski & Darmofal 2009), which seek to adapt the grid with the aim of minimizing numerical errors for a nominal flow condition.

• In the discrete sensitivity framework (such as discrete adjoints, complex step, and finite differences), the grid convergence of nonlinear flow calculations does not guarantee the convergence of linear sensitivities (Giles *et al.* 2003). This attribute has a special relevance in problems involving strong shocks, where the gradient of an output functional of interest may exhibit noise, and hence, cannot be directly utilized. To counter this difficulty, we utilize a bi-grid filtering strategy (Glowinski 1992; Zuazua 2005) that offers the promise of converged linear sensitivities using a discrete computation technique.

In summary, the pursuit of UQ science in hypersonic flow applications, together with sensitivity computations using adjoints, has brought to the table some interesting limitations of the state-of-the-art in adjoint methodologies. In this report, our early work

† FuSim-E project, AIRBUS Spain.

in two novel methodologies is introduced and some preliminary numerical results are presented.

2. Application of adjoint techniques to enhance the computation of response surfaces

In this section, we present a brief introduction to the theoretical basis of the methods that have been developed to improve and accelerate the computation of response surfaces, taking advantage of the adjoint methodology to minimize the numerical error incurred when variations of uncertain input parameters are considered.

2.1. *New "robust" grid methodology*

A response surface represents the explicit dependence of a desired output of a simulation model as a function of all possible values of the decision/input variables. The response surface (Chung & Alonso 2001; Chantrasmi & Iaccarino 2009) is a powerful tool in UQ, although, in practice, a large number of samples is required. Typically these samples constitute small variations of the parameters of interest in some local neighborhood.

We seek to develop a new grid adaptation strategy for creating what we call robust computational grids. Flow computations on these grids must be able to result in low numerical error even if we slightly change the nominal flow conditions (such as the Mach number, geometry, physical constants, etc.) that were used in generating the original adapted grid. The objective is to perform a single grid adaptation about a nominal value of the parameters and to then use this grid for many additional simulations while guaranteeing that the numerical error is held constant. A baseline grid that exhibits this property under reasonable variations of the input parameters is called a robust grid.

In the following discussion, the basis for error estimation in integral outputs (functionals) of partial differential equations (Giles & Pierce 2001; Venditti & Darmofal 2002; Park 2003; Fidkowski & Darmofal 2009) are reviewed. It is well known that this local error estimate could be used as an adaptation indicator in a grid adaptive strategy for producing specially tuned grids for accurately estimating some functional.

Let us consider a fine grid Ω_h and a coarse grid Ω_H. The goal is to obtain an accurate estimate of some functional $f_h(U_h)$ in the fine grid without solving the flow or adjoint equations on the fine grid. An expansion of $f_h(U_h)$ about the coarse-grid solution is

$$f_h(U_h) = f_h(U_h^H) + \left.\frac{\partial f_h}{\partial U_h}\right|_{U_h^H} \left(U_h - U_h^H\right) + H.O.T., \tag{2.1}$$

where U_h^H represents the coarse-grid solution expressed on the fine-grid via some consistent interpolation operation. The nonlinear residual operator representing the flow system of equations is denoted by

$$R_h^U(U_h) = 0. \tag{2.2}$$

Linearizing the residual about the coarse-grid solution yields

$$R_h^U(U_h) = R_h^U(U_h^H) + \left.\frac{\partial R_h^U}{\partial U_h}\right|_{U_h^H} \left(U_h - U_h^H\right) + H.O.T., \tag{2.3}$$

where, neglecting the high order terms, we can write

$$\left(U_h - U_h^H\right) = -\left(\left.\frac{\partial R_h^U}{\partial U_h}\right|_{U_h^H}\right)^{-1} R_h^U(U_h^H). \tag{2.4}$$

Now we define the linear adjoint residual operator $R_h^\Psi(\Psi)$ as

$$R_h^\Psi(\Psi) \equiv \left(\left.\frac{\partial R_h^U}{\partial U_h}\right|_{U_h^H}\right)^T \Psi - \left.\frac{\partial f_h}{\partial U_h}\right|_{U_h^H}, \tag{2.5}$$

where it is important to note that in this last expression we are using a prolongated solution U_h^H to evaluate the Jacobian. By definition $R_h^\Psi(\Psi_h) = 0$, and hence,

$$\left(\left.\frac{\partial R_h^U}{\partial U_h}\right|_{U_h^H}\right)^T \Psi_h = \left.\frac{\partial f_h}{\partial U_h}\right|_{U_h^H}. \tag{2.6}$$

Introducing (2.6) and (2.4) into (2.1) we finally obtain the following expression for the estimate of the numerical error:

$$\epsilon\left(U_h, U_H\right) = f_h(U_h^H) - f_h(U_h) = (\Psi_h)^T R_h^U(U_h^H). \tag{2.7}$$

Unfortunately, to evaluate this last expression it is necessary to solve the adjoint problem (2.6) on the fine grid. The next step is to look for a more appropriate way for estimating the error. Defining Ψ_h^H as the coarse-grid adjoint solution expressed on the fine grid via some consistent projection operation, the error can be written as

$$\epsilon\left(U_h, U_H\right) = (\Psi_h^H)^T R_h^U(U_h^H) + (\Psi_h - \Psi_h^H)^T R_h^U(U_h^H), \tag{2.8}$$

where the difference $(\Psi_h - \Psi_h^H)$ can be estimated using (2.6), and using $R_h^\Psi(\Psi_h) = 0$ we finally obtain

$$\epsilon\left(U_h, U_H\right) = (\Psi_h^H)^T R_h^U(U_h^H) + \left(R_h^\Psi(\Psi_h^H)\right)^T \left(\left.\frac{\partial R_h^U}{\partial U_h}\right|_{U_h^H}\right)^{-1} R_h^U(U_h^H). \tag{2.9}$$

Once again, using (2.4) it is possible to write the error estimation in the following useful form:

$$\epsilon\left(U_h, U_H\right) = (\Psi_h^H)^T R_h^U(U_h^H) + \left(R_h^\Psi(\Psi_h^H)\right)^T \left(U_h - U_h^H\right). \tag{2.10}$$

This expression can be used to generate specially tuned grids for accurately estimating the error in calculating a functional. Note that the first term on the right hand side of the above equation is known via coarse-grid computations and fine-grid interpolations. Previous work (Fidkowski & Darmofal 2009; Venditti & Darmofal 2002) has successfully used this expression to help guide the mesh adaptation process. Our aim is to introduce an adaptation technique that produces low numerical error for a range of variation in some flow or geometric parameters.

The first step in the new methodology is to define a robust grid as a grid in which, for small variations of the solution, the numerical error is nearly constant. In other words, the variation of the numerical error with respect to variations of a parameter k (geometric or flow properties of the problem), must be small or zero in the ideal scenario. The derivative of the numerical error (2.10) owing to a variation of the parameter k can be evaluated as

$$\frac{d\epsilon}{dk} = \left(\frac{d\Psi_h^H}{dk}\right)^T R_h^U(U_h^H) + (\Psi_h^H)^T \frac{dR_h^U(U_h^H)}{dk}$$

$$+\left(\frac{dR_h^{\Psi}(\Psi_h^H)}{dk}\right)^T (U_h - U_h^H) + \left(R_h^{\Psi}(\Psi_h^H)\right)^T \frac{d(U_h - U_h^H)}{dk}, \tag{2.11}$$

where the adjoint and the flow solutions are functions of the parameter k. The value of $(U_h - U_h^H)$ can be estimated using (2.4) to obtain

$$\frac{d\epsilon}{dk} = (\Psi_h^H)^T \frac{dR_h^U(U_h^H)}{dk} + \left(\left(\frac{d\Psi_h^H}{dk}\right)^T - \left(\frac{dR_h^{\Psi}(\Psi_h^H)}{dk}\right)^T \left(\frac{\partial R_h^U}{\partial U_h}\bigg|_{U_h^H}\right)^{-1}\right) R_h^U(U_h^H)$$
$$+\left(\frac{d(U_h - U_h^H)}{dk}\right)^T R_h^{\Psi}(\Psi_h^H). \tag{2.12}$$

In the limit of an extremely well adapted mesh for the direct and adjoint problems, we expect that $R_h^{\Psi}(\Psi_h^H) \approx 0$ and $R_h^U(U_h^H) \approx 0$. In that situation, the variation of the error due to a change in the parameter k can be computed as

$$\frac{d\epsilon}{dk} = (\Psi_h^H)^T \frac{dR_h^U(U_h^H)}{dk}. \tag{2.13}$$

The key idea of this development is that if we adapt the computational grid for solving the direct and the adjoint problems independently, the last expression gives us a very easy way to compute the numerical error when we change the flow conditions to determine the complete response surface. Furthermore, supposing that V_H is the new solution on the coarse grid, and Ψ_H the adjoint solution in the original problem, the correction to the functional value can be computed as

$$\epsilon(V_H) - \epsilon(U_h, U_H) = (\Psi_h^H)^T \left(R_h^V(V_h^H) - R_h^U(U_h^H)\right). \tag{2.14}$$

Using (2.10), the error of the new solution can be computed as

$$\epsilon(V_H) = (\Psi_h^H)^T R_h^V(V_h^H) + \left(R_h^{\Psi}(\Psi_h^H)\right)^T (U_h - U_h^H) \approx (\Psi_h^H)^T R_h^V(V_h^H), \tag{2.15}$$

where it is important to note that this error does not depend on the finest grid solution. In principle, for a reconstruction-based finite volume scheme, the numerical error is likely to change even when the solution is slightly perturbed by a change in input conditions. Fortunately, this error can be estimated using coarse-grid calculations. On the other hand, if we have Galerkin orthogonality, the first term in (2.10) will be zero and the adapted grid (for the adjoint and flow problem) will provide excellent results even when some flow parameter is slightly changed.

The adaptation technique that we have developed is based in obtaining $R_h^{\Psi}(\Psi_h^H) \approx 0$ and $R_h^U(U_h^H) \approx 0$ for the baseline flow solution. To achieve this objective, it is natural to employ a residual-based indicator to drive the flow and adjoint adaptation process. Either of the following approaches can be pursued:

- A direct approach, which consists of computing the value of $R_h^{\Psi}(\Psi_h^H)$ and $R_h^U(U_h^H)$ in a very fine grid and subsequently adapting the original grid in zones where these values are large.
- An indirect strategy, in which the residual is driven to zero in the dual control volumes of the grid. Note that the original numerical scheme is designed to have a zero flow residual on the primal control volumes.

Once we have an estimation of the residual for the direct and adjoint problems, it can be used as an indicator for mesh adaptation. With regard to the refinement process itself (Borouchaki *et al.* 2005), there is only one element subdivision that can preserve

the element shape quality: homothetic subdivision, which for a planar triangle, splits it into four by adding three new vertices at the middle of the edges. It has to be noted that elements that share these edges must also be divided if hanging nodes are to be avoided.

In the residual based strategy we typically define the error as

$$e = |\Omega|^{\alpha} \sqrt{R_{\rho}^2 + R_{\rho\vec{v}}^2 + R_{\rho E}^2}, \tag{2.16}$$

where $|\Omega|$ is the area of the control volume, and R_i are the four (two-dimensional) or five (three-dimensional) residuals at each node. A widely used formulation utilizes $\alpha = 1$. The advantage of scaling the indicator with a positive value of α is that the adaptation stops automatically in the corresponding area after several cycles even when discontinuities are present in the flowfield. Finally an indicator of the error is computed as

$$e_{lim} = e_m + c_{lim} e_s, \tag{2.17}$$

where e_{lim} is the error limit, e_m is the mean of the error indicator, e_s is the standard deviation of the error indicator, and c_{lim} is a constant. Typically a value near unity is used for the constant. The homothetic element refinement is used in grid elements where the error indicator is greater than a corresponding error tolerance.

2.2. *Sensitivity computation on small pressure sensor (bi-grid filtering technique)*

It is known that with the discrete sensitivity approach (automatic differentiation, complex step, and finite differences), the convergence of nonlinear flow equations to machine precision does not guarantee the convergence of functional sensitivities (Giles *et al.* 2003). In particular, we have observed that in the presence of strong shocks and for functionals that extend across only a small number of mesh cells, there are significant differences between the gradient of a functional computed with the continuous and the discrete adjoints (or exact finite differences), in that the latter can be expected to be noisy (mainly for functionals with a small spatial footprint).

The use of automatic differentiation (Griewank 2000; Martins *et al.* 2006; Gauger *et al.* 2007; Mader *et al.* 2008) is a very attractive technique to tackle derivative computations when dealing with complex multi-physics systems. However, as we will see, in the presence of strong shocks the computed gradient can be noisy, and this situation has critical relevance if we are interested in computing second derivatives using the same methodology.

To obtain a useful expression to process the discrete sensitivities, the starting assumption is that the continuous adjoint methodology will provide a gradient approximation that will be closer to the analytical gradient (in fact, in the limit of a very fine grid it must be the analytical one). This has been confirmed by performing numerical experiments in flows with strong shocks. Thus, an attempt will be made at building a discrete adjoint that mimics the behavior of the continuous adjoint. Once such a discrete adjoint is constructed, the next step will be to compare this new discrete adjoint with the classical one.

Consider the stationary Euler equations in a domain Ω:

$$R(U) = \vec{\nabla} \cdot \vec{F}(U) = 0, \quad \text{in } \Omega, \tag{2.18}$$

where R is the residual, U is the vector of conservative variables, and $\vec{F}$ is the convective flux vector. The Euler equations have to be completed with the flow tangency boundary condition at all solid walls, and at the inlet and outlet boundary conditions are specified

for incoming waves, while outgoing waves are determined by the solution inside the fluid domain.

In a numerical practice, a modified version of these equations is solved. This modified governing equation can be written as

$$R(U) + D(U) = \vec{\nabla} \cdot \vec{F}(U) + \epsilon \vec{\nabla} \cdot (G(U)\vec{\nabla}U) = 0, \quad \text{in } \Omega, \tag{2.19}$$

where the the stabilizing viscosity term can be interpreted as the discretization of a second derivative $\vec{\nabla}(G(u)\nabla(u))$ for some viscosity function G depending on the particular scheme under consideration, and ϵ contains powers of spatial coordinates. It is important to note that ϵ should approach zero as the grid spacing approaches zero.

If we define a functional $J(U, k)$ that depends on the conservative variables and a parameter k that depends on the flow or geometry, the complete variation of the functional is

$$\delta J = \frac{\partial J}{\partial U}\delta U + \frac{\partial J}{\partial k}\delta k. \tag{2.20}$$

Typically, the discrete adjoint problem will be introduced through the Lagrange multipliers to remove the explicit dependence on δU.

It is important to note that our objective is to compare two discrete adjoints, the classical one and a new discrete adjoint that mimics the continuous adjoint behavior:

- In the classical discrete adjoint approach, the modified state equation (2.19) is fulfilled, and we will build the Lagrangian: $\mathcal{L}(U, k, \lambda^D) = J(U) + \lambda^D [R(U, k) + D(U)]$.
- On the other hand, using ideas inspired in the continuous adjoint problem, we also define the following Lagrangian: $\mathcal{L}(U, k, \lambda^C) = J(U) + \lambda^C [R(U, k) + C]$, where C is a constant which includes high-order terms of the discretization that do not depend on U (in the continuous adjoint procedure).

The variation of the objective function J in these approaches is, therefore

$$\delta J = \frac{\partial J}{\partial U}\delta U + \frac{\partial J}{\partial k}\delta k - \lambda^D \left(\frac{\partial R}{\partial U} + \frac{\partial D}{\partial U}\right)\delta U - \lambda^D \left(\frac{\partial R}{\partial k}\right)\delta k, \tag{2.21}$$

$$\delta J = \frac{\partial J}{\partial U}\delta U + \frac{\partial J}{\partial k}\delta k - \lambda^C \left(\frac{\partial R}{\partial U}\right)\delta U - \lambda^C \left(\frac{\partial R}{\partial k}\right)\delta k. \tag{2.22}$$

The final expressions for the sensitivities hold if λ^D and λ^C satisfy the following adjoint equations:

$$\frac{\partial J}{\partial U} = \lambda^D \left(\frac{\partial R}{\partial U} + \frac{\partial D}{\partial U}\right), \quad \frac{\partial J}{\partial U} = \lambda^C \frac{\partial R}{\partial U}, \tag{2.23}$$

where the classical discrete adjoint can be written as

$$\lambda^D = \frac{\partial J}{\partial U}\left(\frac{\partial R}{\partial U}\right)^{-1} - \lambda^D \frac{\partial D}{\partial U}\left(\frac{\partial R}{\partial U}\right)^{-1}. \tag{2.24}$$

The last step of our formulation involves computing the difference between the discrete adjoint, which mimics the continuous adjoint behavior, and the classical discrete adjoint:

$$\lambda^C = \lambda^D \left(\frac{\partial D}{\partial U}\left(\frac{\partial R}{\partial U}\right)^{-1} + I\right), \tag{2.25}$$

where it must be possible to check that $\frac{\partial D}{\partial U}\left(\frac{\partial R}{\partial U}\right)^{-1}$ is nothing more than a smoother of the continuous adjoint solution.

The main issue appears when we are looking for solutions with strong shocks. In that

situation we hypothesize that this operator produces a strong damping in high frequencies of the continuous adjoint beyond a critical wave number. In other words, the high frequency numerics of the continuous adjoint solution are limited by the dispersion produced by $\frac{\partial D}{\partial U}\left(\frac{\partial R}{\partial U}\right)^{-1}$. The analogy of this problem with other similar problems (Glowinski 1992; Zuazua 2005) suggests a filtering of the high frequencies to eliminate the harmful effect of the smoother described above. This may be done by a bi-grid algorithm.

The bi-grid strategy is a powerful numerical tool that can be used to damp or filter the spurious numerics in control problems. To achive this radical filtering it suffices to define a finite grid of step size $2h$. Following this, the flow solution is approximated in that grid and re-interpolated again to the fine mesh. With this procedure, the short wavelengths are eliminated from the adjoint solution. The major component of the noise was introduced at these scales. Finally, an iterative process is proposed to compute the new discrete adjoint solution

$$\lambda^D_{n+1} = \lambda^C - Filter\left\{\lambda^D_n\left(\frac{\partial D}{\partial U}\left(\frac{\partial R}{\partial U}\right)^{-1}\right)\right\}, where\ \lambda^D_0 = \lambda^C. \tag{2.26}$$

It is important to note that this filtering strategy will be especially useful if we are interested in computing sensitivities on small sensors or for second derivatives.

2.3. *Continuous Euler adjoint formulation for two-dimensional hypersonic problems*

The sensitivity computation in internal aerodynamics problems is formulated on a fluid domain Ω, enclosed by boundaries divided into a inlet S_{in}, outlet S_{out}, and solid wall boundaries S_{wall}. The objective is to compute the variation of

$$J = \int_{S\in S_{wall}} j(P, \vec{n}_S)\, ds, \tag{2.27}$$

with respect to changes in the geometry and inlet flow. It is important to note that $j(P, \vec{n}_S)$ is a function that depends on $\vec{n}_S$ (inward-pointing unit normal to S) and the pressure P.

Hypersonic inviscid flows are characterized by the appearance of strong shock discontinuities Σ. If the the discontinuity touches the surface S and $x_b = \Sigma \cap S$ we have that, in order to account for discontinuities (Bardos & Pironneau 2002) in the variation of J,

$$\begin{aligned}\delta J = &\int_S \left[\frac{\partial j}{\partial P}\partial_n P + \vec{t}\cdot\partial_{tg}\left(\frac{\partial j}{\partial \vec{n}_S}\right) - \kappa\left(j + \frac{\partial j}{\partial \vec{n}_S}\vec{n}_S\right)\right]\delta S\, ds \\ &+ \int_{S\setminus x_b}\frac{\partial j}{\partial P}\delta P\, ds - \frac{[j]_{x_b}}{\vec{n}_S\cdot\vec{t}_\Sigma}\left[\delta\Sigma(x_b) - (\vec{n}_S\cdot\vec{n}_\Sigma)\,\delta S(x_b)\right].\end{aligned} \tag{2.28}$$

Ideal fluids are governed by the Euler's equations (introduced in the previous section) that can develop strong shock waves. When this occurs, the Rankine-Hugoniot conditions $\left[\vec{F}\cdot\vec{n}_\Sigma\right]_\Sigma = 0$ relate the flow variables on both sides of the discontinuity.

In the presence of shock discontinuities the formal linearization of the state equations fails to be true (Baeza *et al.* 2009) and the sensitivity of the model needs to take into account perturbations of the solution and perturbations of the location of the shock. In this case, δU stands for the infinitesimal change in the state on both sides of the discontinuity and results from the solution of the linearized Euler equations, whereas $\delta\Sigma$ describes the infinitesimal normal deformation of the discontinuity and it results from a linearization of the Rankine-Hugoniot conditions:

$$
\begin{array}{ll}
\vec{\nabla}\cdot\left(\vec{A}\,\delta U\right)=0, & \text{in } \Omega\setminus\Sigma,\\
\delta\vec{v}\cdot\vec{n}_S=-\delta S\,\partial_n\vec{v}\cdot\vec{n}_S+\left(\partial_{tg}\delta S\right)\vec{v}\cdot\vec{t}_S, & \text{on } S_{wall}\setminus x_b,\\
(\delta W)_+=\delta W_{in}, & \text{on } S_{in},\\
(\delta W)_+=0, & \text{on } S_{out},\\
\left[\vec{A}(\delta\Sigma\,\partial_n U+\delta U)\right]_\Sigma\cdot\vec{n}_\Sigma+\left[\vec{F}\right]_\Sigma\cdot\delta\vec{n}_\Sigma=0 & \text{on } \Sigma,
\end{array}
\tag{2.29}
$$

with $(\delta W)_+$ representing the incoming characteristics and where $\partial\vec{F}/\partial U=\vec{A}$ is the Jacobian matrix. In order to eliminate δP and $\delta\Sigma$ from (2.28), the adjoint problem is introduced through Lagrange multipliers Ψ^T

$$
\begin{array}{ll}
-\vec{A}^T\cdot\vec{\nabla}\Psi=0, & \text{in } \Omega\setminus\Sigma,\\
\vec{\varphi}\cdot\vec{n}_S=\frac{\partial j}{\partial U}, & \text{on } S_{wall}\setminus x_b,\\
\Psi^T(\vec{A}\cdot\vec{n}_S)_-=0, & \text{on } S_{in}\cup S_{out},\\
\left[\Psi^T\right]_\Sigma=0,\quad \partial_{tg}\Psi^T\left[\vec{F}\cdot\vec{t}_\Sigma\right]=0, & \text{on } \Sigma,\\
\Psi^T(x_b)\left[\vec{F}\cdot\vec{t}_\Sigma\right]_{x_b}=\frac{[j]_{x_b}}{n_S\cdot\vec{t}_\Sigma}, & \text{at } x_b.
\end{array}
\tag{2.30}
$$

The procedure is as follows: first the linearized Euler equations and Rankine-Hugoniot conditions are multiplied by the adjoint variables. Then, the result is integrated over the domain (taking care of the discontinuities), and finally the result is added to (2.28). Upon identifying the corresponding terms in that final expression with the adjoint equations, we can write the variation of the functional as:

$$
\begin{aligned}
\delta J=&\int_S\left[\frac{\partial j}{\partial P}\partial_n P+\vec{t}\cdot\partial_{tg}\left(\frac{\partial j}{\partial\vec{n}_S}\right)-\kappa\left(j+\frac{\partial j}{\partial\vec{n}_S}\vec{n}_S\right)\right]\delta S\,ds\\
&+\int_{S\setminus x_b}\left[\left(\partial_n\vec{v}\cdot\vec{n}_S\right)\vartheta+\partial_{tg}\left(\left(\vec{v}\cdot\vec{t}_S\right)\vartheta\right)\right]\delta S\,ds\\
&+\int_{S_{in}}\Psi^T(\vec{A}\cdot\vec{n}_S)\,\delta U_{in}\,ds+[j(P)]_{x_b}\frac{\vec{n}_S\cdot\vec{n}_\Sigma}{\vec{n}_S\cdot\vec{t}_\Sigma}\delta S\,(x_b)\,,
\end{aligned}
\tag{2.31}
$$

where κ is the surface curvature, $\vec{\varphi}=(\psi_2,\psi_3)$ and $\vartheta=\rho\psi_1+\rho\vec{v}_S\cdot\vec{\varphi}+\rho H\psi_4$. Using (2.30) and (2.31) we are able to compute any variation of J due to a geometrical or inlet flow change, even when the computation of J includes a shock discontinuity impinging on the surface of integration S. Note that the importance of some of these terms depends on the actual flow condition and, in particular, on the relative angle of impingement of the discontinuity on the surface S.

While not explicitly used in the results presented here, this derivation is meant to suggest that care must be exercised to ensure that terms in adjoint solutions that include discontinuities are accounted for carefully. Within the context of actual flow discretizations, discontinuities are represented by regions of high gradients. Therefore, the importance of all terms must be carefully assessed.

3. Numerical experiments

In this section a selection of preliminary numerical results are shown. Two geometries (involving single and multiple shock reflections in a constant area channel) have been selected as baseline configurations. Inviscid simulations at high Mach number and

FIGURE 1. Density contours for nominal conditions (Mach number 4.0 and ramp angle 6.0°)

FIGURE 2. Adjoint density contours for nominal conditions and pressure sensor located in the lower wall

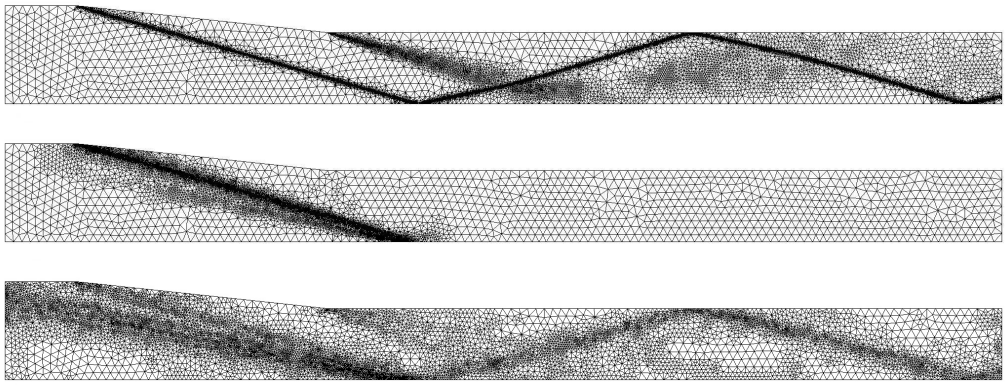

FIGURE 3. Grid adaptation using a gradient-based method (upper), adjoint-based computable error (middle) and the new robust method (lower)

functionals defined over small patches of the solid wall will be common aspects of the simulations that we have performed.

3.1. *Robust grid adaptation*

To study the applicability of this method, a two-dimensional Euler supersonic test case has been selected. In particular, we are interested in creating a robust grid for the Clemens configuration (Wagner *et al.* 2007).

The nominal conditions (as in the experiments) are an inlet Mach number of 5.0 and a ramp angle 6.0° (Fig.1). The sensitivity computation (Fig.2) has been performed using a second-order continuous adjoint solution. The objective of this test is to verify if the grid adapted (using the new robust technique) for those nominal conditions also provides a good value of the objective function for the complete response surface.

The baseline grid has a total of $1,356$ nodes and $2,450$ triangular elements. The total length of the setup is 333.0 mm, and the pressure sensor is located on the lower wall at 116.08 mm from the inlet (the size of the pressure sensor is 5.08 mm).

In order to compare the performance of different grid adaptation techniques (Fig.3)

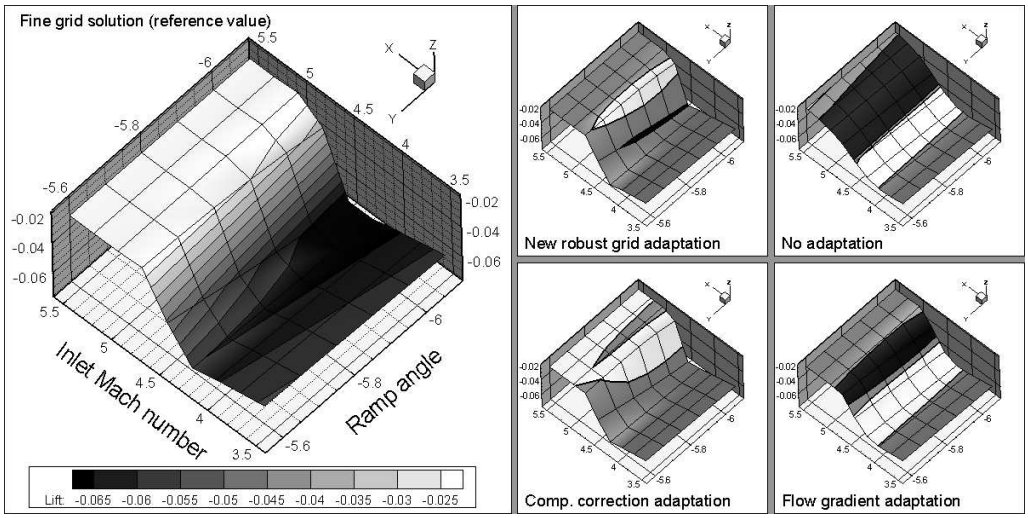

FIGURE 4. Comparison between different adaptation strategies (grey color signifies an error $< 4.0\%$)

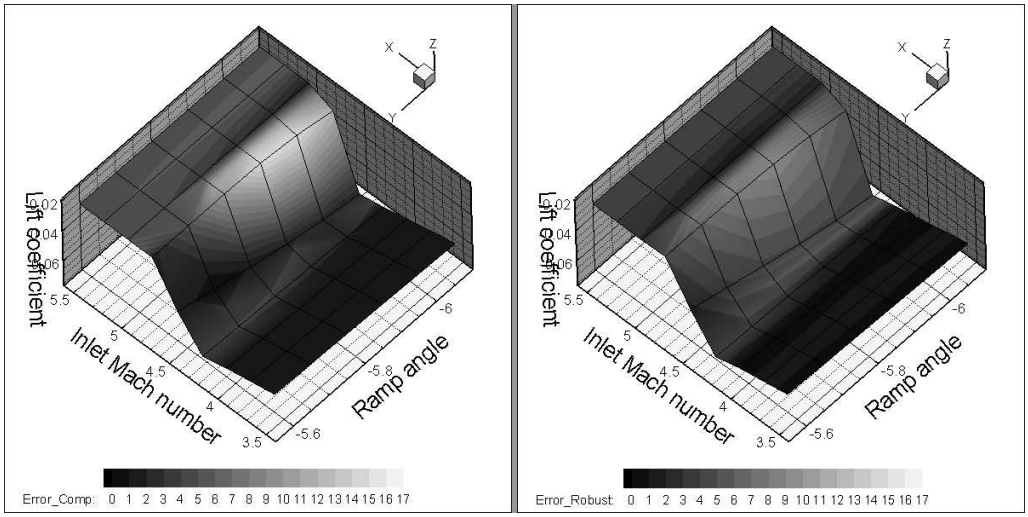

FIGURE 5. Direct comparison between computable error based adaptation and "robust" grid adaptation

we have used three different error indicators: gradient based, classical adjoint based (computable error), and the new robust adaptation method.

Once the adaptation is completed, the final step consists of computing the entire response surface (Fig.4) and comparing the results with the response surface that has been computed using a very fine reference grid (Fig.5). In conclusion, for the complete response surface computation, the robust grid strategy provides a lower error compared with other techniques, despite the fact that only one adaptation around Mach 5.0 and ramp angle 6.0° is used.

FIGURE 6. Density contours of the supersonic ramp

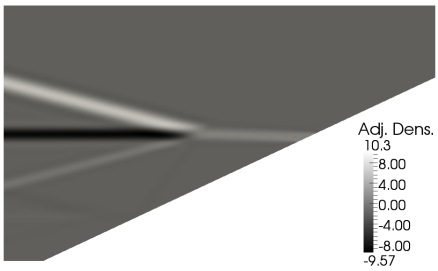

FIGURE 7. Adjoint density contours of the supersonic ramp; note that the sensor is located where the adjoint solution reaches it maximum value at the solid wall

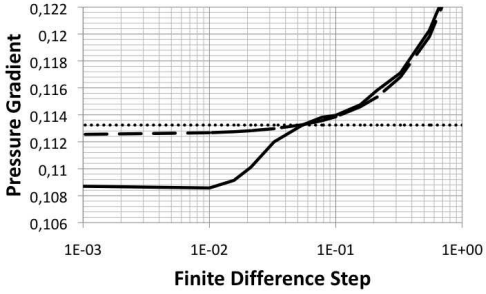

FIGURE 8. Comparison between continuous adjoint sensitivity and finite-difference technique on a baseline grid (continuous adjoint ····· ; finite differences ——— ; finite differences with bi-grid – – –)

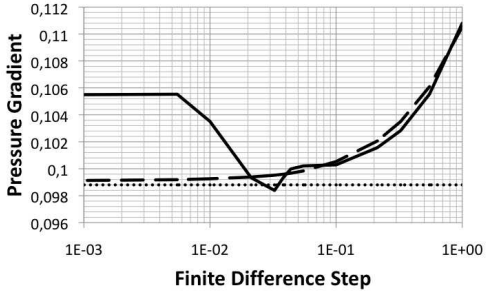

FIGURE 9. Comparison between continuous adjoint sensitivity and finite-differences technique on a very fine grid (continuous adjoint ····· ; finite differences ——— ; finite differences with bi-grid – – –)

3.2. *Bi-grid filtering technique on a supersonic ramp*

To study the applicability of the bi-grid filtering technique, a two-dimensional Euler supersonic ramp of 25° (Fig.6) is selected. In particular, we are interested in the derivative, with respect to the inlet Mach number, of the pressure on a small sensor located approximately in the middle of the ramp.

With the use of a fourth-order dissipation-based discretization, the continuous adjoint (Fig.7) sensitivity was confirmed to be within 0.1% of the analytical sensitivity. Similarly, the discrete adjoint sensitivity was confirmed to exactly match the finite-difference value for a small enough finite difference step size. For comparison purposes, we use finite differences to approximate the discrete sensitivity, and the bi-grid technique are applied to the solution of the direct problem.

The convergence of the finite-difference sensitivity is shown for two different grids: baseline grid (Fig.8) with $5,680$ nodes, Mach number 4.3, and a very fine grid (Fig.9) with $22,472$ nodes, Mach number 4.1. It is interesting to note that the finite-difference approach shows a strange behavior near the analytical value of the gradient, beyond which it does not converge to the analytical value of the gradient (represented by the continuous adjoint solution). Once the bi-grid technique is applied to the flow solution, we obtain a value for the discrete sensitivity that is very similar to the analytic one.

4. Future plans and conclusions

In this work we proposed and showed preliminary results for two new adjoint-based techniques that were aimed at enhancing the computation of response surfaces and flow sensitivities.

• We have demonstrated that by adapting the computational grid using a residual-based strategy for the flow and the adjoint solutions, one can obtain a robust grid with respect to small variations of the flow parameters. Further work will be required to incorporate anisotropic adaptation, develop sensors to estimate the strength of adaptation, and obtain rigorous upper bounds for the error estimation.

• We have also proposed a method to filter the flow solution with the aim of obtaining noise-free sensitivities using discrete techniques. This bi-grid strategy is expected to be especially useful for flows with strong shocks and for objective functions that are defined over a small portion of the computational boundary. Further work must be done in order to understand the behavior of the filtering operator. Current tests are underway in testing this within the framework of Automatic Differentiation (AD).

Acknowledgments

This work was supported by the U.S. Department of Energy under the Predictive Science Academic Alliance Program (PSAAP). The first author was visiting the Aero/Astro Department at Stanford University while this work was performed. He also thanks Prof. E. Zuazua for helpful discussions.

REFERENCES

Anderson, W. K. & Venkatakrishnan, V. 1997 Design optimization on unstructured grids with a continuous adjoint formulation. AIAA Paper 97-0643.

Baeza, A., Castro, C., Palacios, F. & Zuazua, E. 2009 2-D Euler shape design on nonregular flows using adjoint Rankine-Hugoniot relations. *AIAA J.* **47** (3), 552–562.

Bardos, C. & Pironneau, O. 2002 A formalism for the differentiation of conservation laws. *C. R. Acad. Sci., Paris* **I** (335), 839–845.

Borouchaki, H., Villard, J., Laug, P. & George, P. L. 2005 Surface mesh enhancement with geometric singularities identification. *Comput. Methods Appl. Mech. Engrg.* **194**, 4885–4894.

Castro, C., Lozano, C., Palacios, F. & Zuazua, E. 2007 A systematic continuous adjoint approach to viscous aerodynamic design on unstructured grids. *AIAA J.* **45** (9), 2125–2139.

Chantrasmi, T. & Iaccarino, G. 2009 Computing shock interactions under uncertainty. AIAA Paper 2009-2284.

Chung, H. S. & Alonso, J. J. 2001 Using gradients to construct response surface models for high-dimensional design optimization problems. AIAA Paper 2001-0922.

Eldred, M. S. 2009 Recent advances in non-intrusive polynomial chaos and stochastic collocation methods for uncertainty analysis and design. AIAA Paper 2009-2274.

Fidkowski, K. J. & Darmofal, D. L. 2009 Output-based error estimation and mesh adaptation in computational fluid dynamics: overview and recent results. AIAA Paper 2009-1303.

Gauger, N. R., Walther, A., Moldenhauer, C. & Widhalm, M. 2007 Automatic

differentiation of an entire design chain for aerodynamic shape optimization. *New Res. in Num. and Exp. Fluid Mech.* **96**, 454–451.

Giles, M. B., Duta, M. C., Müller, J.-D. & Pierce, N. A. 2003 Algorithm developments for discrete adjoint methods. *AIAA J.* **41** (2), 198–205.

Giles, M. B. & Pierce, N. A. 2001 Adjoint error correction for integral outputs. *Tech. Rep.* 01/18. Oxford University Computing Laboratory, Numerical Analysis Group, Oxford, England.

Glowinski, R. 1992 Ensuring well-posedness by analogy; Stokes problem and boundary control for the wave equation. *J. of Comp. Phys.* **103**, 189–221.

Griewank, A. 2000 *Evaluating derivatives, principles and techniques of algorithmic diferentiation*. Society for Industrial and Applied Mathematics, Philadelphia.

Jameson, A. 1988 Aerodynamic design via control theory. *J. Sci. Comput.* **3**, 233–260.

Kim, S., Alonso, J. J. & Jameson, A. 2002 Design optimization of high-lift configurations using a viscous continuous adjoint method. AIAA Paper 2002-0844.

Mader, C. A., Martins, J. R. R. A., Alonso, J. J. & van der Weide, E. 2008 ADjoint: an approach for rapid development of discrete adjoint solvers. *AIAA J.* **46** (4), 863–873.

Martins, J. R. R. A., Mader, C. A. & Alonso, J. J. 2006 ADjoint: an approach for rapid development of discrete adjoint solvers. AIAA Paper 2006-7121.

Mavriplis, D. J. 2006 Multigrid solution of the discrete adjoint for optimization problems on unstructured meshes. *AIAA J.* **44** (1), 42–50.

Nadarajah, S. K. & Jameson, A. 2000 A comparison of the continuous and discrete adjoint approach to automatic aerodynamic optimization. AIAA Paper 2000-0667.

Park, M. A. 2003 Three-dimensional turbulent rans adjointbased error correction. AIAA Paper 2003-3849.

Pierce, N. A. & Giles, M. B. 2002 Adjoint and defect error bounding and correction for functional estimates. *J. of Comp. Phys.* **200**, 769–794.

Venditti, D. A. & Darmofal, D. L. 2002 Grid adaptation for functional outputs: application to two-dimensional inviscid flows. *J. of Comp. Phys.* **176**, 40–69.

Wagner, J. L., Valdivia, A., Yuceil, K. B., Clemens, N. T. & Dolling, D. S. 2007 An experimental investigation of supersonic inlet unstart. AIAA Paper 2007-4352.

Zuazua, E. 2005 Propagation, observation, control and numerical approximation of waves approximated by finite difference method. *SIAM Review* **47** (2), 197–243.